Received: 2 July 2021 | Revised: 31 January 2022 | Accepted: 17 March 2022

DOI: 10.1002/poc.4346

RESEARCH ARTICLE

Journal of Physical Organic Chemistry WILEY

Experimental and theoretical investigation on the thermal isomerization reaction of tristriazolotriazines

Matthias Jochem | **Daniel Limbach** | **Stefan Glang** | **Tobias Haspel** | **Heiner Detert**

Department for Organic Chemistry, Johannes Gutenberg-University Mainz, Mainz, Germany

Correspondence
H. Detert, Department for Organic Chemistry, Johannes Gutenberg-University Mainz, Duesbergweg 10–14, 55099, Mainz, Germany.
Email: detert@uni-mainz.de

Funding information
Johannes Gutenberg-Universität Mainz

Abstract

The isomerization of tristriazolotriazione with tangential substituents to radial isomers occurs in a cascade of three ring opening/rotation/ring closure steps of the central triazine. Donor substitution accelerates the isomerization which can be catalyzed by Brønsted acids. The velocity of the rearrangements drops with each step by a factor of 4, whereas the gain in heat of formation increases. Density functional theory (DFT) calculations led to transition states; their energies correspond to the experimental data. Threefold isomerization strongly affects the mesomorphic properties.

KEYWORDS

discotic liquid crystal, DFT calculation, heterocycles, kinetics, mesomorphism, rearrangement

1 | INTRODUCTION

Tristriazolotriazine **1** (TTT, Scheme 1), a planar, C_3-symmetrical heterocycle, is known since 1911 (R = NH_2)[1] but has been overlooked for more than 90 years, except a single comment on the structure.[2] Huisgen, as part of his studies on tetrazole chemistry,[3] reported the synthesis of a TTT **2** (R = phenyl).[4] Both tetracyclic isomers are composed of 1,2,4-triazoles annulated to a central 1,3,5-triazine. Both structures are C_3-symmetrical, but the orientation of the substituents is either "radial" for isomer **1** or "tangential" for type **2**. In 2008, the tristriazolotriazine **2** was recognized as core for discotic liquid crystals[5,6] and a series of mesomorphous TTTs with a broad range of thermal and optical properties has been reported since Cristiano et al..[7] In addition to the often very broad mesophases with clearing temperatures up to 232°C, TTTs apparently have a high thermal stability.[8] Despite the high nitrogen content of the core, thermogravimetric analysis (TGA) shows weight loss only above 400°C.[6] Nevertheless, repeated differential scanning calorimetry (DSC) measurements in the range T = 20–260°C of mesomorphous alkoxyphenyl-TTTs **2** (R = dialkoxyphenyl) gave decreasing transition temperatures, indicating a change in the chemical composition of the material (Scheme 1). Tartakovsky[9] has shown that TTT **2** (R = phenyl) isomerizes at 360°C to a mixture of nonsymmetrical isomers and proposed a Dimroth rearrangement-like mechanism[10] for this transformation. In the course of this rearrangement, the triazole annulation pattern changes, bringing the tangentially oriented substituents (type **2**) to radial positions (type **1**). Under less forcing conditions, the controlled thermal treatment of TTTs was developed as a successful

Dedicated to Prof. Dieter Lenoir on the occasion of his 85th birthday.

method to convert tangentially substituted *t*-TTTs **2** to radially substituted *r*-TTTs **1.**[11] With the exception of two, all known *r*-TTTs have been prepared on this route.[7e,11,12] The aim of this study is to shed light on the mechanism of the rearrangement, factors determining the ease of the conversion, and methods to accelerate the tangential-radial reorganization.

2 | RESULTS AND DISCUSSION

2.1 | Synthesis

The Huisgen procedure is the only route to *t*-TTTs.[4] The 5-substituted tetrazoles **3** were dissolved in xylene with collidine as a base, and after equilibration, cyanuric chloride was added. The mixture was heated for an appropriate time to 80–120°C, and the product was isolated via column chromatography on silica gel (Scheme 1). The *t*-TTTs **2a**–**2f** for this study are substituted with groups of different donor quality (Table 1). Preparative details and analytical data are given in the supporting information (SI) (**2a**, **2c**, and **2f,** p. 7–11) and in Rieth et al..[7f]

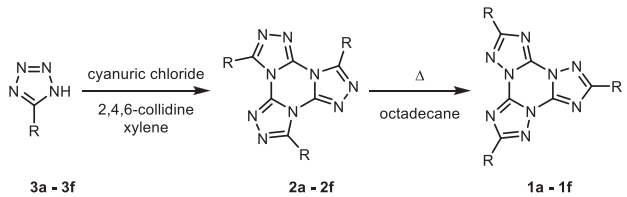

SCHEME 1 *C* $_3$-symmetrical TTTs **1**, **2,** and synthesis of **2**

2.2 | Thermal rearrangement

The structural rearrangement of *t*-TTTs to their *r*-isomers involves three isomerization steps; less symmetrical isomers with mixed *r*- and *t*-annulation appear as distinct intermediates (Scheme 2).[9,11]

The harsh conditions (360°C) applied by Tartakovsky are not suitable for alkoxyphenyl substituted TTTs due to carbonization. At lower temperatures ($T < 275$°C) and in an inert solvent, quantitative *t*-to-*r*-rearrangements are possible. For instance, the thermal treatment of **2e** in octadecane solution at 235°C proceeds within 330 h from pure *t*-TTT via nonsymmetrical isomers (*rtt*-TTT and *rrt*-TTT) to pure **1e** with three radially oriented substituents. NMR spectra following the course of this process are collected in Figure 1. The signal of the aromatic proton on **2e** ($\delta = 7.43$) shifts to $\delta = 7.64$ for the isomer **1e**. The appearance and vanishing of further aromatic proton signals prove the existence of intermediate isomers. Within the first 16 h, the starting material **2e** is completely consumed and even the first intermediate ($\delta = 7.37$, 7.55, 7.66) is gone after 41 h. But the transformation of the second intermediate ($\delta = 7.44$, 7.46, 7.64) requires more than 200 h. Small variations in the chemical shift δ are due to concentration changes[13]; higher concentrations shift the aromatic signals to higher field; this effect is much more pronounced for radial isomers ($\Delta\delta \leq 0.1$ ppm).

As the concentration of **2e** in the initial phase decreased rapidly, a second isomerization experiment was conducted at 195°C. As above, the cascade of rearrangements was monitored by NMR spectroscopy over 34 days. The molar fractions of starting material *all-t*-TTT **2e** (black), intermediates *rtt*-TTT and *rrt*-TTT

Entry	R	Yield (%)	m.p. (°C)
2a	Undecyl	59	48
2b	4-tridecyloxyphenyl	90	78
2c	4-(2-ethylhexyloxy)-2,5-dimethylphenyl	72	184
2d	3,4-di (tridecyloxy)phenyl	48	74
2e	3,4,5-tri (hexyloxy)phenyl	92	117
2f	4-N,N-di (dodecyl)aminophenyl	72	128

TABLE 1 Synthesis of *t*-TTTs

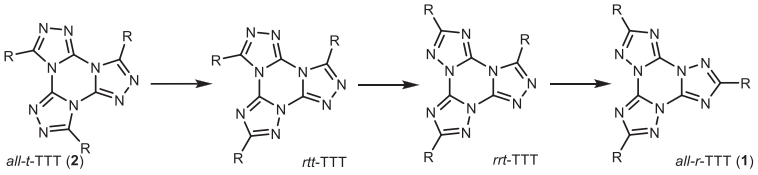

SCHEME 2 Structural changes during isomerization of *t*-TTTs **2** to *r*-TTTs **1**

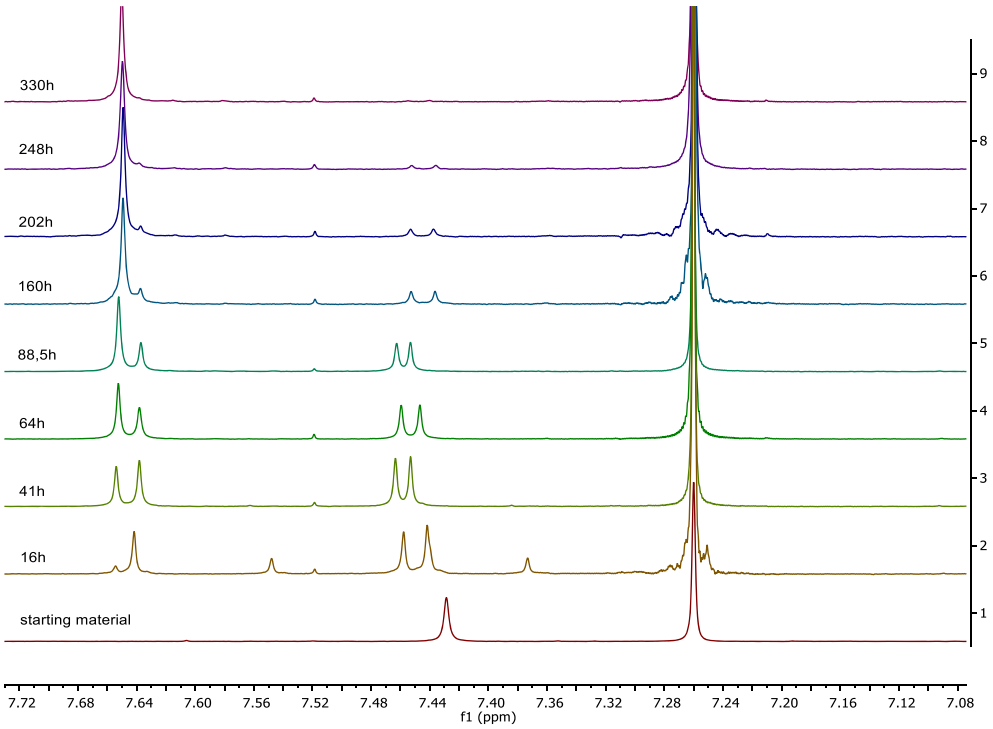

FIGURE 1 H-NMR spectra (400 MHz, $CDCl_3$, 25°C) monitoring the thermal isomerization of **2e** to **1e** (octadecane, 235°C), only low-field region shown

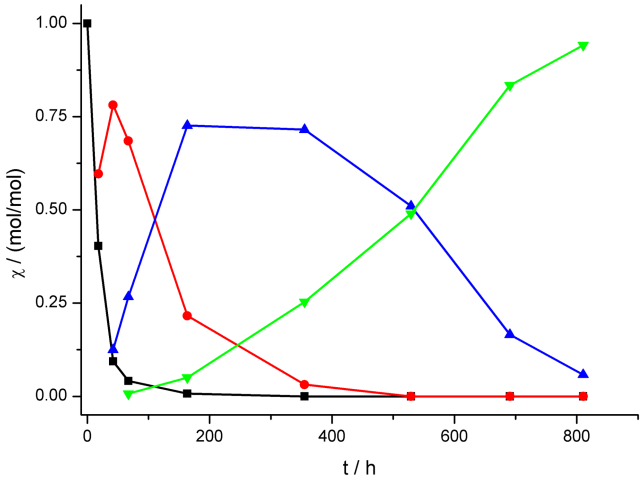

FIGURE 2 Molar fraction of involved compounds during the isomerization at 195°C black: **2e**, red first intermediate, blue: second intermediate, green: **1e**

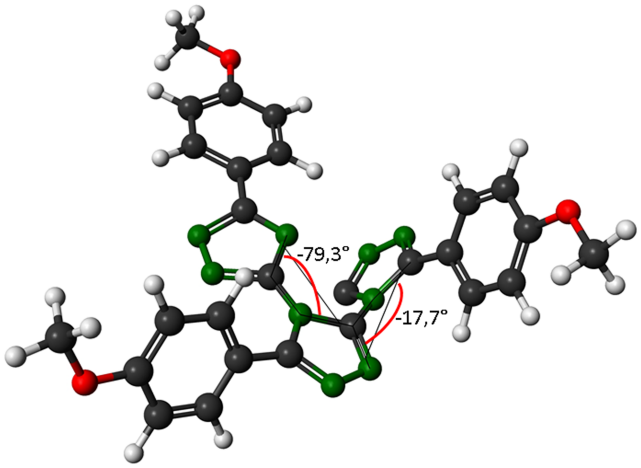

FIGURE 3 Transition state of the first rearragenment according to AM1 calculations

(red and blue), and the final *all-r*-TTT **1e** (green) are given in Figure 2.

The diagram shows that the isomerization is very fast in the beginning and becomes slower in the end. An interesting fact is that the reaction becomes kinetically slower with every step. The integration of the curves in Figure 3 allows to give a relative persistence of the individual compounds and therefore a sequence of relative rate constants. The ratio of the integral mole fractions over time corresponds to the ratio of the inverse rate constants (see SI, p. 20). The first isomerization step occurs with a rate constant about 4.5 times higher than the second and nearly 16 times higher than the rate constant of the third step! Density functional theory (DFT) calculations had shown that the first rearrangement stabilizes the TTT by 8.3 kcal/mol and the second and third by 12.3 kcal/mol each.[11] A comparison of these data and the relative rate constant shows that this sequence of closely related rearrangements does not follow the Bell–Evans–Polanyi principle since the fastest reaction correlates with the smallest reaction enthalpy.

NMR spectroscopy clearly revealed that the *t-r*-rearrangement of TTTs occurs in three consecutive steps. Besides the rare case of a dyotopic rearrangement,[14] the process could be a threefold sequence of triazine ring opening, rotation of a terminal triazole around the triazole-triazole bond, and ring closure.[9,11] The triazine bond fission can be either homolytic or heterolytic.

2.3 | Substituent effect on the isomerization

In a series of rearrangement reactions of **2a**–**2f** (octadecane, 235°C), the progress was monitored by NMR after 5 and 10 h. The initial rate of the thermal isomerization of *t*-TTTs increases with the electronic donor effect of the substituent on the TTT. Alkyl substituted TTT (**2a**) is less reactive than TTTs with alkoxyphenyl (**2b** and **2c**). More prone to rearrangement are dialkoxyphenyl and trialkoxyphenyl TTTs (**2d** and **2e**), while the amino-*t*-TTT **2f** is the by far most reactive compound. As this sequence correlates with the donor effect, either a destabilizing effect of the electron-donating groups on the triazine C-N bond or, more probable, a stabilizing effect on the ring-opened intermediates facilitates the disruption of the triazine. This suggests a polar mechanism with a positively charged triazole unit. However, since the change of solvent from nonpolar octadecane to very polar NMP provokes only a marginal speeding up of the rearrangement, a polar mechanism is not supported. On the other hand, equimolar amounts of the radical scavenger additives triphenylmethane and hydroquinone had similarly weak but opposite effects on the rearrangement of **2e**. With triphenylmethane, a slightly decelerated, but with hydroquinone, a slightly accelerated reaction was observed. As the biradical generated by a homolytic ring opening should have a lifetime sufficient for a reaction with the radical trapping reagent and no open-chain tristriazoles have been observed, this route can be excluded.

The slightly accelerated rearrangement of **2e** in the presence of hydroquinone indicates a polar interaction since hydroquinone is not only a radical scavenger but also a Brønstedt acid. A heterolytic fission of a triazine C-N bond can be supported by interaction with acids or nucleophiles; the possible pathway for interaction with a phenol can be protonation of the TTT or attack of the phenolate as nucleophile.

As a consequence, we investigated the action of several nucleophilic and acidic additives on **2e** in octadecane solution; the molar ratio of TTT and additive was about 1 to 10. The presence of stearic acid on the thermal reaction (235°C) of 2**e** provoked a fast decomposition. According to NMR and mass spectra, the action of stearic acid destroys the tristriazolotriazine nucleus, and the formation of triazolones and triazolyl triazolones as well as a stearyl triazolyl triazole is suggested from mass spectroscopy. It is known that the action of hydrochloric acid on triphenyl-TTT (**1**, R = phenyl) leads to related triazolone fragments.[9] Supposedly, the stearic acid protonates the TTT core and the carboxylate adds to central C-N bond followed by ring opening (nucleophilic substitution) or the stearate adds, after ring opening, to the cationic terminus of the tris-triazole chain (Scheme 3). In a following syn-elimination of hexadecyl ketene, a terminal triazolone is formed. Nucleophilic substitutions on the 3-position of 1,2,4-triazoles[15] and the formation of triazolone via ketene elimination[16] have been reported earlier. Further similar degradation reactions lead to the mononuclear and dinuclear triazolones.

Change from stearic acid to benzoic acid effectuates a completely different outcome. Benzoic acid expedites the rearrangement without formation of the triazolone products of decomposition. These findings prove the role of the acid as catalyst and the α-methylene group as origin for the decomposition pathway via ketene

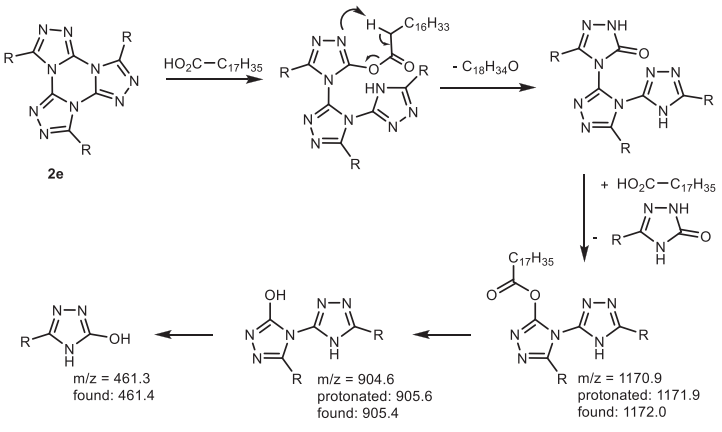

SCHEME 3 Degradation of the TTT nucleus in the reaction with stearic acid

syn-elimination. The role of the proton, not the nucleophile, is confirmed by experiments with trihexylamine and tris-cyclohexyl phosphine as nucleophilic additives. These rearrangements occur with the same rate as in the absence of additives.

With the addition of benzoic acid, better is trimethyl benzoic due to the lower volatility, a significant acceleration of the rearrangement was observed. Since 4-bromobenzoic acid, and even more tetrabutylammonium hydrogen sulfate, provoke a higher increase in rate, pKa appears to be a rate-determining factor. The results of a comparative study on acid-catalyzed isomerization on some *t*-TTTs are collected in Table 2. The noncatalyzed isomerization cascade of **2e** requires 333 h for completeness (entry 1), but in the presence of *p*-bromobenzoic acid, the same result is obtained in only 22 h (entry 4). *t*-TTT with only one alkoxy group (**2c**, entry 3) rearranges with a comparable reaction rate, but **2a**, lacking the donor group, requires 42 h, nearly double in time. The reaction rate of **2e** in the presence of acid (entry 4) is very close to the rate of amino-TTT **2f** in the absence of acid (entry 5). Addition of acid to this compound has a detrimental effect on the reaction time—the isomerization is decelerated by a factor of 7. Here, protonation occurs on the amino group thus inhibiting a charge transfer from the amino to the cationic triazole terminus. This stabilization appears to be very efficient; it competes with the effect of protonation on alkoxy substituted TTTs and, in combination with the high temperature (235°C), is probably the reason for a partial dealkylation.

From these data, we derived that the mechanism of the isomerization reaction contains a heterolytic ring opening (Scheme 4) which can be accelerated either by electron-donating substituents R or through a protonation at the triazine-nitrogen. A homolytic bond breaking plays, if at all, a minor part.

2.4 | Theoretical investigation

In addition to the experimental results, DFT calculations should illuminate the isomerization process from a theoretical point of view. DFT calculations[17] were performed to find the energetic positions of the four tristriazolotriazines (*all-t*, *rtt*, *rrt*, *all-r*) and the transition states of the reaction path connecting these isomers. Since nearly all experimental isomerizations had been performed on electron-rich alkoxyaryl-TTTs, tris (4-methoxyphenyl)-*t*-TTT (**2**, R = *p*-methoxyphenyl) was chosen, ensuring the electron-rich character while keeping the atom count rather low. Semiempirical methods (MO-G/AM1)[18,19] were used to get an initial glance on possible structural features of assumed zwitterionic transition states based on Grimme's general proceeding.[20] To achieve this, for each isomerization step, one C-N bond in the triazine ring was removed and the two connecting bonds were rotated by their dihedral angle in steps of 5–15° for a full rotation. These preliminary studies discovered local saddle points for perpendicular disconnected triazoles and a transition state; the latter was formed by rotation of one phenyltriazolyl unit around a triazole-triazole bond, while the other triazoles remained in an almost coplanar geometry.

DFT calculations using the B88LYP functional and 6-31G(d,p) basis set[21–25] were performed according to the structures obtained by semiempirical methods. Hence, starting geometries for DFT calculations were generated by ring opening and rotating the triazole group with the supposed negative charge from previously

TABLE 2 Impact of acid catalysis on isomerization of TTTs at 235°C

	Substituent at the TTT core	Additive	Time (h)
1	3,4,5-trihexyloxyphenyl **2e**		333
2	undecyl **2a**	4-Br-C_6H_4COOH	42
3	2,5-dimethyl-4-(2-ethylhexyloxy)phenyl **2c**	4-Br-C_6H_4COOH	23
4	3,4,5-trihexyloxyphenyl **2e**	4-Br-C_6H_4COOH	22
5	4-(N,N-dodecylamino)phenyl **2f**		23
6	4-(N,N-dodecylamino)phenyl **2f**	4-Br-C$_6$H4COOH	163

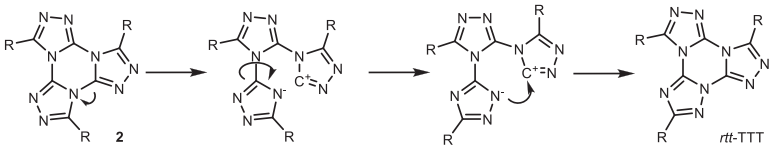

SCHEME 4 Detailed reaction mechanism with ionic ring opening

optimized structures[11] to a dihedral angle of 90° between the disconnected rings. This led finally to a transition state for the second step of the rearrangement cascade. Deducing the similarity of all three steps, starting geometries for the other two steps were adapted accordingly. These structures led to transition states connecting the local minima. All calculated transition states showed quite similar singular negative eigenvalues in the hessian matrix, indicated by an imaginary IR frequency of about 490–529 cm^{-1}. Intrinsic reaction pathway calculations accordingly showed appropriate ring-closing movements following the indicated eigenmodes.

In the next step, all structures of the reaction coordinate were refined by optimization in orca (4.2.1)[26–28] at the B3LYP/def2-SVP[29–32] level of theory, with a fine grid being necessary for smooth convergence. Transition states were checked for single imaginary modes. These imaginary eigenmodes of TS1, TS2, and TS3 were found to correspond with frequencies of −582, −582, and −594 cm^{-1}. Previously reported structures[11] were recalculated to fit the much finer grid and update of software version. (For comparison between results at different levels of theory, see supporting information).

The energy differences of the starting material and the intermediates and final product were calculated to be −9.5, −18.9, and −32.3 kcal/mol, respectively. Regarding the transition states, the calculated reaction barriers were found to be 64.7, 68.9, and 72.5 kcal/mol for the three consecutive steps (Figure 4). This sequence is in accordance with the experimental data. Nevertheless, we cannot exclude that other intermediates and transition states of higher energy may occur.

Regarding the second rearrangement step, two possible ring openings on intermediate IM1 (*rtt*-TTT) are

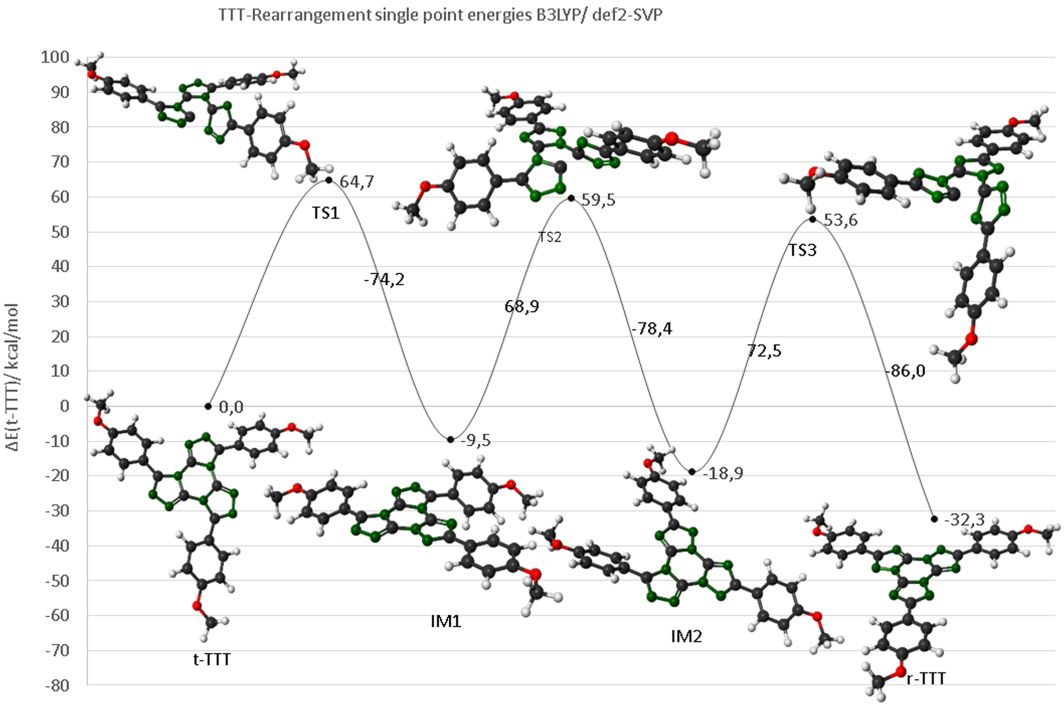

FIGURE 4 Calculated reaction coordinates for the complete rearrangement cascade. All values given in kcal/mol

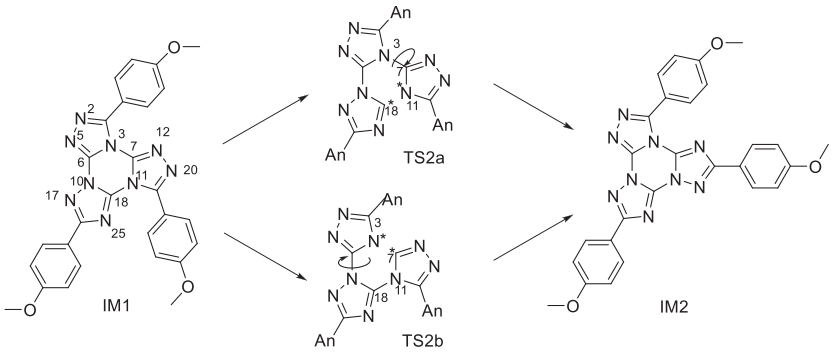

SCHEME 5 Two different pathways for the second rearrangement step

theoretically possible. They lead via two different transition states (TS2a and TS2b; Scheme 5) to a single second rearranged product IM2 (*rrt*-TTT). Both dissociation of bond N3-C7 and of bond N11-C18 would formally enable the next rearrangement. These pathways were investigated in the DFT studies by breaking the respective bond and searching for transition states. It was found that only in the first case saddle points on the PES could be located and verified on multiple runs from various starting points, differing in the angle and the distance of the disconnected rings. We propose therefore that the ring opening occurs only on the side of the already "rearranged nitrogen," for example, the dissociation of the bond N3-C7 (Figure 5). QTAIM (Quantum Theory of Atoms in Molecules) Analysis[33,34] of the results showed that the bond N3-C7 is 1.395 Å long, while the bond N11-C18 is significantly shorter (1.391 Å). In addition, the neighboring N10-C18 bond of the rearranged r-triazole measures only 1.369 Å, whereas the C7-N11 bond of the still t-annulated triazole is much longer: 1.398 Å. The analysis also showed that the triazole C-N bond lengths at the annulated positions vary with the isomerization: The first rearranged bond is only 1.369 Å, whereas the r-TTT shows mean lengths of 1.379 Å. t-triazole units in contrast have a mean length of 1.392 Å. The mean bond length between triazoles is shortened by about 0.011 Å by full rearrangement (see SI for graphics and full lists, p. 48-66).

For all obtained transition states, the common features are approximate distances of the cationic carbon (C4 in TS2 and C6 in TS3, Figure 6) to the carbon of the rotating anionic ring (C2 in TS2 and C4 in TS3) of about 1.69–1.76 Å and a similar distance to one of the neighboring nitrogen atoms (N3 in TS2 and N5 in TS3) in the assumable negatively charged triazole of about 1.7 to 1.8 Å. All three triazole rings are planar in themselves but tilted towards each other as indicated by the dihedral angles (114.2° and 38.1° in TS2). The ring with the positive charge is almost perpendicular to the negatively charged triazole. Hence, the transition state might include a cation–π interaction.

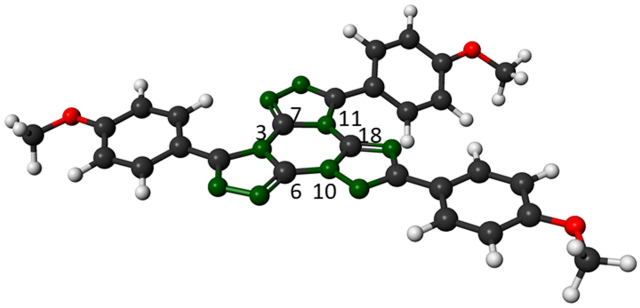

FIGURE 5 rtt-TTT with numbered TTT core as starting point for second rearrangement step

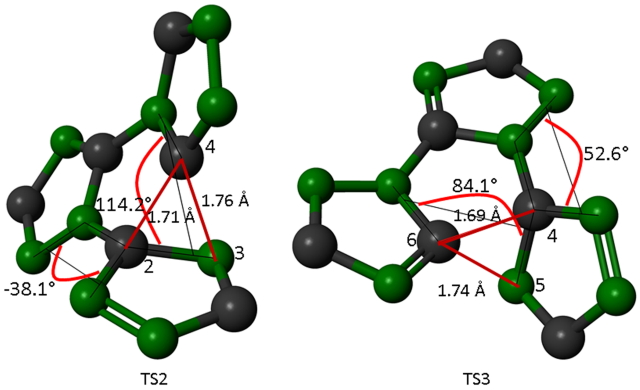

FIGURE 6 TTT core during transition state of the second (TS2, left) and third (TS3, right) rearrangement

2.5 | Mesomorphous properties of compounds under investigation

Tristriazolotriazines with one alkyl chain per arm are not mesomorphous, but two or three chains of medium length in the 3,4-positions or 3,4,5-positions are good prerequisites for liquid crystallinity.[7e,f] Accordingly, *t*-TTTs **2a–2c** are not mesomorphous but **2d** and **2e** are (Table 3). In spite of the swallow-tail side chain[16] *N*,*N*-di(dodecyl)amino, **2f** is not mesomorphous. The structural change from paddle-wheel (*t*-TTT **2**) to propeller shape (*r*-TTT **1**) has a strong impact on the thermal behavior. The width of the LC phase of **2d** shrinks upon *t*-*r* isomerization to **1d**; this is due to both higher melting point and lower clearing temperature. However, the opposite is true for the trihexyloxy TTTs **2e**/**1e**. The melting point of the radial isomer **1e** is about 100°C lower than of the *t*-isomer, but the effect on the clearing temperature appears to be small. X-ray diffraction of these compounds reveals the typical hexagonal columnar arrangement in the LC phase with a higher order for the radial isomer **1e**.

TABLE 3 Transition temperatures for selected compounds

	Substitution	T/°C (ΔH/kJmol^{-1})
2d	3,4-$OC_{13}H_{27}$	Cr 74 (12.4) M 175 (6.1) I
1d	3,4-OC13H_{27}	Cr 94 (16.8) M 119 (9.9) I
2e	3,4,5-OC_6H_{13}	Cr 116 (19.9)Colhd 184 (4.6) I
1e	3,4,5-OC_6H_{13}	Cr 13 (8.9) Colh 180 (POM) I

Notes: Colh(d), columnar hexagonal (disordered); Cr, crystalline; I, isotropic phase; M, mesophase; POM, clearing point observed by polarization optical microscopy.

3 | CONCLUSION

Thermal isomerization *t*-TTTs brings substituents from tangential to radial positions, changing the shape of the molecules from paddle-wheel to propeller, and has a strong impact on mesomorphic properties. This alteration of shape modifies the mesomorphic properties in an unpredictable manner. The whole process consists in a threefold sequence of triazine ring opening, triazole rotation, triazine ring closure steps, and the rate constants increase with gradual transformation. Electron-pair donating groups on the TTT alleviate the reaction, and protonation on the triazole ring accelerates the isomerization. Structures of transition states were obtained by DFT calculations; their energies correlate with the reaction rates.

ACKNOWLEDGMENT

Open access funding enabled and organized by Projekt DEAL.

DATA AVAILABILITY STATEMENT

Data are available in the article supporting information.

ORCID

Matthias Jochem https://orcid.org/0000-0003-3159-5038

Heiner Detert https://orcid.org/0000-0001-6910-8173

REFERENCES

[1] a) K. A. Hofmann, O. Ehrhart, *Ber. Dtsch. Chem. Ges.* **1911**, *44*, 2713. b) K. A. Hofmann, O. Erhart, *Ber. Dtsch. Chem. Ges.* **1912**, *45*, 2731.

[2] D. W. Kaiser, G. A. Peters, V. P. Wystrach, *J. Org. Chem.* **1953**, *18*, 1610.

[3] R. Huisgen, J. Sauer, H. J. Sturm, J. H. Markgraf, *Chem. Ber.* **1960**, *93*, 2106.

[4] R. Huisgen, H. J. Sturm, M. Seidel, *Chem. Ber.* **1961**, *94*, 1555.

[5] S. Glang, V. Schmitt, H. Detert, *Proc. 36th Ger. Top. Meeting on LCs* **2008**, *125*.

[6] R. Cristiano, H. Gallardo, A. J. Bortoluzzi, I. H. Bechtold, C. E. M. Campos, R. L. Longo, *Chem. Commun.* **2008**, *46*, 5134.

[7] a) R. Cristiano, J. Eccher, I. H. Bechtold, C. N. Tironi, A. A. Vieira, F. Molin, H. Gallardo, *Langmuir* **2012**, *28*, 11590; b) T. Rieth, T. Marszalek, W. Pisula, H. Detert, *Chemistry* **2014**, *20*, 5000; c) S. Glang, T. Rieth, D. Borchmann, I. Fortunati, R. Signorini, H. Detert, *Eur. J. Org. Chem.* **2014**, 3116; d) A. G. Dal-Bó, G. G. L. Cisneros, R. Cercena, J. Mendes, L. M. de Silveira, E. Zapp, K. G. Dominicano, R. da Costa Duarte, F. S. Rodembusch, T. E. A. Frizon, *Dyes Pigments* **2016**, *135*, 49; e) H. Detert, *Eur. J. Org. Chem.* **2018**, 4501; f) T. Rieth, N. Tober, D. Limbach, T. Haspel, M. Sperner, N. Schupp, P. Wicker, S. Glang, M. Lehmann, H. Detert, *Molecules* **2020**, *25*, 5761. https://doi.org/10.3390/molecules25235761 g) C. P. Umesh, A. T. M. Marcelis, H. Zuilhof, *Liq. Cryst.* **2015**, *42*, 1269; h) S. Wang, X. Wang, K. H. Lee, S. Liu, J. Y. Lee, W. Zhu, Y. Wang, *Dyes Pigments* **2020**, *182*, 108589. i) S. K. Pathak, Y. Xiang, M. Huang, T. Huang, X. Cao, H. Liu, G. Xie, C. Yang, *RSC Adv.* **2020**, *10*, 15523.

[8] Q. Zeng, Y. Qu, J. Li, H. Huang, *RSC Adv.* **2016**, *6*, 5419.

[9] V. A. Tartakovsky, A. E. Frumkin, A. M. Churakov, Y. A. Strelenko, *Russ. Chem. Bull. Int. Ed.* **2005**, *54*, 719.

[10] O. Dimroth, *Liebigs Ann. Chem.* **1909**, *364*, S. 183.

[11] T. Rieth, N. Röder, M. Lehmann, H. Detert, *Chem. Eur. J.* **2018**, *24*, 93.

[12] W. Weissflog, A. Wiegeleben, S. Diele, D. Demus, *Crystal Res. Technol.* **1984**, *19*, 583.

[13] A. Mitra, P. J. Seaton, R. A. Assarpour, T. Williamson, *Tetrahedron* **1998**, *54*, 15489.

[14] a) M. T. Reetz, *Angew. Chem. Int. Ed.* **1971**, *11*, 129. bL. A. Paquette, G. A. O'Doherty, R. D. Rogers, *J. Am. Chem. Soc.* **1991**, *113*, 7761.

[15] a) W. Maes, B. Verstappen, W. Dehaen, *Tetrahedron* **2006**, *62*, 2677; b) T. P. Kofman, I. V. Vasil'eva, M. S. Pevzner, *Chem. Heterocycl. Compd.* **1976**, *12*, 1061; c) J. L. Miller, T. J. Church, D. Leonoudakis, K. Lariosa-Willingham, N. L. Frigon, C. S. Tettenborn, J. R. Spencer, J. Punnonen, *Mol. Pharmacol.* **2015**, *88*, 357.

[16] G. Young, H. Annable, *J. Chem. Soc.* **1897**, *71*, 200.

[17] DFT Calculations Were Performed Using SCIGRESS Version FJ 2.9.1 (EU 3.4.3) Employing the DGauss Software With the 6-31G** Basis Set. Pictures Were Created Using SCIGRESS Software.

[18] MO-G Version FJ 2.9.1 (EU 3.4.3) From SCIGRESS Suite by Fujitsu.

[19] M. J. S. Dewar, E. G. Zoebisch, E. F. Healy, J. J. P. Stewart, *J. Am. Chem. Soc.* **1985**, *107*(13), 3902.

[20] S. Dohm, M. Bursch, A. Hansen, S. Grimme, *J. Chem. Theory Comput.* **2020**, *16*, 2002.

[21] A. D. Becke, *Phys. Rev. A* **1988**, *38*, 3098.

[22] C. Lee, W. Yang, R. G. Parr, *Phys. Rev. B* **1988**, *37*, 785.

[23] W. J. Hehre, R. Ditchfield, J. A. Pople, *J. Chem. Phys.* **1972**, *56*, 2257.

[24] R. Ditchfield, W. J. Hehre, J. A. People, *J. Chem. Phys.* **1971**, *54*, 724.

[25] P. C. Hariharan, J. A. Pople, *Theoret. Chim. Acta* **1973**, *28*, 213.

[26] F. Neese, *Wiley Interdiscip. Rev.: Comput. Mol. Sci.* **2012**, *2*(1), 73.

[27] F. Neese, *Wiley Interdiscip. Rev.: Comput. Mol. Sci.* **2017**, *8*, e1327.

[28] F. Neese, F. Wennmohs, A. Hansen, U. Becker, *Chem. Phys.* **2009**, *356*, 98.

[29] A. D. Becke, *J. Chem. Phys.* **1993**, *98*, 5648.

[30] P. J. Stephens, F. J. Devlin, C. F. Chablowski, M. J. Frisch, *J. Phys. Chem.* **1994**, *98*, 11623.

[31] R. H. Hertwig, W. Koch, *Chem. Phys. Lett.* **1997**, *268*, 345.

[32] F. Weigend, R. Ahlrichs, *Phys. Chem. Chem. Phys.* **2005**, *7*, 3297.

[33] T. Liu, F. Chen, *J. Comput. Chem.* **2012**, *33*, 580.

[34] T. Lu, F. Chen, *J. Mol. Graph. Model.* **2012**, *38*, 314.

SUPPORTING INFORMATION

Additional supporting information may be found in the online version of the article at the publisher's website.

How to cite this article: M. Jochem, D. Limbach, S. Glang, T. Haspel, H. Detert, *J Phys Org Chem* **2022**, *35*(7), e4346. https://doi.org/10.1002/poc.4346